

RESEARCH

Open Access



# A newly developed deep learning-based system for automatic detection and classification of small bowel lesions during double-balloon enteroscopy examination

Yijie Zhu<sup>1,2,3†</sup>, Xiaoguang Lyu<sup>1,2,3†</sup>, Xiao Tao<sup>1,2,3</sup>, Lianlian Wu<sup>1,2,3</sup>, Anning Yin<sup>1,2,3</sup>, Fei Liao<sup>1,2,3</sup>, Shan Hu<sup>4</sup>, Yang Wang<sup>1,2,3</sup>, Mengjiao Zhang<sup>1,2,3</sup>, Li Huang<sup>1,2,3</sup>, Junxiao Wang<sup>1,2,3</sup>, Chenxia Zhang<sup>1,2,3</sup>, Dexin Gong<sup>1,2,3</sup>, Xiaoda Jiang<sup>1,2,3</sup>, Liang Zhao<sup>1,2,3\*</sup> and Honggang Yu<sup>1,2,3\*</sup>

## Abstract

**Background** Double-balloon enteroscopy (DBE) is a standard method for diagnosing and treating small bowel disease. However, DBE may yield false-negative results due to oversight or inexperience. We aim to develop a computer-aided diagnostic (CAD) system for the automatic detection and classification of small bowel abnormalities in DBE.

**Design and methods** A total of 5201 images were collected from Renmin Hospital of Wuhan University to construct a detection model for localizing lesions during DBE, and 3021 images were collected to construct a classification model for classifying lesions into four classes, protruding lesion, diverticulum, erosion & ulcer and angioectasia. The performance of the two models was evaluated using 1318 normal images and 915 abnormal images and 65 videos from independent patients and then compared with that of 8 endoscopists. The standard answer was the expert consensus.

**Results** For the image test set, the detection model achieved a sensitivity of 92% (843/915) and an area under the curve (AUC) of 0.947, and the classification model achieved an accuracy of 86%. For the video test set, the accuracy of the system was significantly better than that of the endoscopists (85% vs.  $77 \pm 6\%$ ,  $p < 0.01$ ). For the video test set, the proposed system was superior to novices and comparable to experts.

**Conclusions** We established a real-time CAD system for detecting and classifying small bowel lesions in DBE with favourable performance. ENDOANGEL-DBE has the potential to help endoscopists, especially novices, in clinical practice and may reduce the miss rate of small bowel lesions.

**Keywords** Double-balloon enteroscopy, Artificial intelligence, Small bowel

<sup>†</sup>Yijie Zhu and Xiaoguang Lyu contributed equally to this work.

\*Correspondence:

Honggang Yu  
yuhonggang@whu.edu.cn  
Liang Zhao  
airmanzhao@whu.edu.cn

Full list of author information is available at the end of the article



## Background

Double-balloon enteroscopy (DBE) is important for managing small bowel disease [1]. Different from capsule endoscopy (CE), DBE not only serves as a diagnostic tool but allows for tissue sampling and therapeutic intervention [2, 3]. DBE has a real-time image reading mode. However, there are inherent oversight and distraction risks in the use of this mode due to its time-consuming and technically demanding nature. Additionally, diagnosis is influenced by endoscopist experience variability. It has been previously reported that the first DBE procedures yielded false-negative results in 20–23.8% of patients [4–7]. The lesion types missed during these procedures include ulcers, diverticulum, tumours, and vascular lesions [6]. As immediate repeat inspection is not routine for DBE, missed lesions are unlikely to be detected during the same procedure. This will delay the detection and treatment of bleeding lesions, which increases the risk of recurrent bleeding and repeat examinations [6].

Artificial intelligence (AI) has become a strong focus of interest in clinical practice, owing to its potential to reduce diagnostic errors and manual workload [8–12]. Convolutional neural networks (CNNs) have been used for big data analysis of medical images [9, 13–21]. CNN-based algorithms have displayed outstanding performance in gastrointestinal endoscopy that is comparable to or even superior to that of experts [22–26]. AI may assist in diagnosis during endoscopic examinations by automatically detecting, characterizing, measuring, and localizing various lesions. Computer-aided diagnostic (CAD) systems could improve the examination quality and diagnostic accuracy in gastrointestinal endoscopy, helping clinicians formulate therapeutic strategies and prognosis predictions [27–30]. Recently, there has been overwhelming literature supporting the crucial role of CNNs on CE to automatically recognize classify, and localize small bowel abnormalities [31–43]. However, there is little research on the detection and classification of DBE.

In this study, we aim to develop a CNN-based system for automatically detecting multiclass small bowel lesions in both DBE images and videos. This system might increase the diagnostic yield for small bowel lesions that are responsible for gastrointestinal bleeding and reduce the burden of repeat DBE.

## Methods

### Study design and datasets

#### Study design

This study aims to build a deep learning system named ENDOANGEL-DBE for detecting and classifying small

bowel lesions in DBE. This is a retrospective, single-centre, and diagnostic study.

ENDOANGEL-DBE is composed of two models. Model 1 is responsible for detection, and Model 2 is responsible for classification (diverticulum, protruding lesion, erosion & ulcer, angioectasia). ENDOANGEL-DBE will give results on the lesion location and type in real time during DBE.

The individual performance of the two models was tested by evaluating two image test sets separately and ENDOANGEL-DBE was tested through the evaluation of 65 videos and compared to 8 human observers, including 4 novices and 4 experts.

#### Datasets

All images and videos for training and testing were retrospectively collected from Renmin Hospital of Wuhan University (RHWU). Images that revealed the characteristics of small bowel lesions were included in this study.

The Model 1 training set included 5201 images, with 4201 abnormal images as positive samples and 1000 normal images as noise, from 463 patients from November 1st, 2016 to October 30th, 2020 (Supplementary Table 1).

The Model 1 image test set included 915 abnormal images from 98 patients and 1318 normal images from 89 patients from November 1st, 2020 to June 15th, 2021 (Supplementary Table 1).

The Model 2 training set included 3021 abnormal images from 389 patients from November 1st, 2016 to October 30th, 2020. A total of 4171 lesion images were abstracted for Model 2 training according to the standard answer, i.e., the consensus of three experts (Supplementary Table 2).

The Model 2 image test set included 915 abnormal images from 98 patients, which were the same as the abnormal images in the Model 1 image test set. A total of 1422 lesion images were abstracted for Model 2 training according to the standard answer (Supplementary Table 2).

The Video test set was collected from June 16th, 2021 to November 12th, 2021. The Video test set contained 65 video clips from 30 consecutive patients, including 2 with diverticulum, 30 with protruding lesions, 25 with erosions and ulcers, and 8 with angioectasia. The average length of the videos was  $66.29 \pm 21.14$  seconds. Each video clip was used to extract consecutive images at a rate of 25 frames per second (Supplementary Table 3).

All images were obtained from DBE (EN-450 T5, EN-530 T; Fujifilm, Tokyo, Japan) and video systems (VP-4450HD; Fujifilm, Tokyo, Japan). There was no overlap of patients between the training and test sets.

**Development of the CAD system**

**Image processing**

All the black frames in the original images were automatically cropped according to pixel changes. Moreover, the training set was enhanced by rotating, transforming, resizing, and cropping.

**Experts reached a consensus on the standard answer of the images**

Three experts (L Zhao, A Yin, and F Liao) reached a consensus to obtain the standard answer for training and testing. If more than two experts came to the same conclusion for a given image, the conclusion was the standard answer; otherwise, the experts discussed their findings and reached a consensus. The experts, with more than 200 cases of DBE experience, were all from RHWU. They labeled images by bounding each lesion with the smallest rectangular box that enclosed the lesion through an online annotator [44], and the labels were the standard answer for training and testing Model 1. Then, they classified all images into diverticulum, protruding lesion, erosion & ulcer, and angioectasia as the standard answer for training and testing Model 2.

Protruding lesions included: polyps, nodules, epithelial tumours, submucosal tumours, and venous structures. Erosions and ulcers were classified into the same

category. Erosions, ulcers, and diverticulum included lesions of various aetiologies. Angioectasia included Yano–Yamamoto classification types 1a and 1b.

**Construction of the CAD system**

The CAD system consisted of two CNNs. The structure of ENDOANGEL-DBE is shown in Fig. 1. You only look once (YOLO) [45] was used for detection (Model 1). YOLO is a region-based object detector that uses a single CNN to detect lesion regions. YOLO has been trained for lesion detection in digestive endoscopic examinations and is widely used in studies for its fast and accurate detection [46–48]. ResNet-50 [49], a residual learning framework with good generalizability, was used to build Model 2. The residual blocks of ResNet-50 utilize skip connections to avoid vanishing gradients. The dataset was trained in Google’s TensorFlow. Mode l tuning was used for training. The model tuning parameters are shown in Supplementary Table 4. Dropout, data augmentation, and early stopping with patience of val\_loss were used to lower the overfitting risk (Supplementary Tables 5 to 6).

The threshold value of Model 1 was set to 0.02 according to the ROC curve. Because Model 2 was a four-type classification model, the label with the highest threshold value and with a threshold value  $\geq 0.25$  among the four

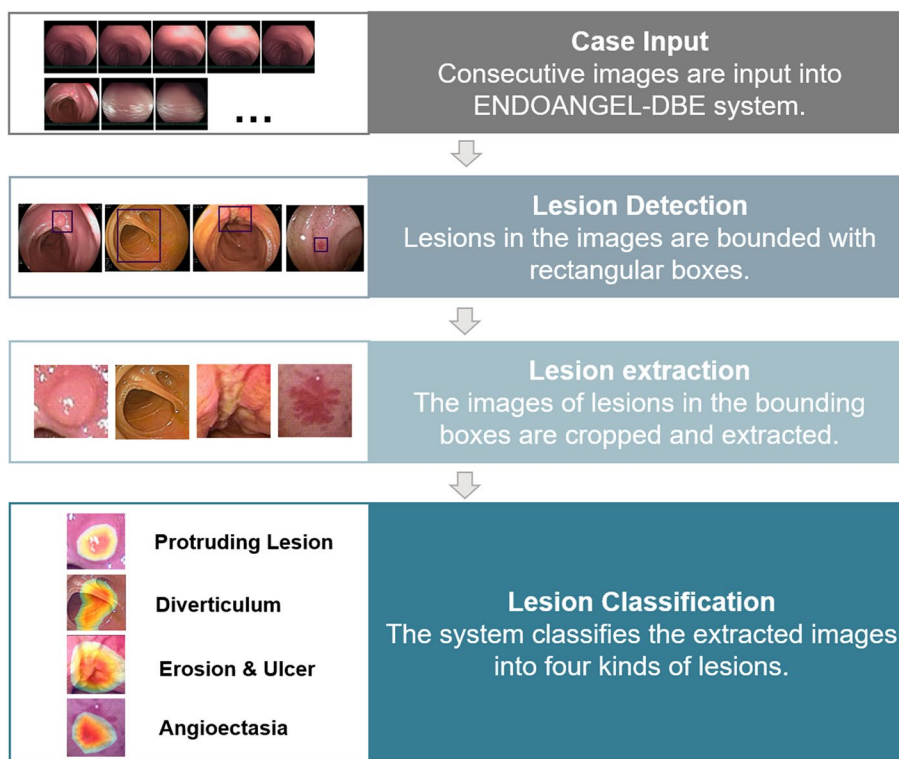


**Fig. 1** Processing flow diagram of ENDOANGEL-DBE

classification labels assigned to the target image was the final classification that the model outputs.

**Training and testing**

The training and testing flow chart is shown in Fig. 2 and the dataset distribution is shown in Supplementary Tables 1 to 3. We evaluated the individual performance of the two models with the image test set and the overall performance of ENDOANGEL-DBE with the video test set. In addition, ENDOANGEL-DBE performance was compared with endoscopists' performance for the video test set.

**Assessment with image test sets**

**Assessment of YOLO**

The area under the receiver operating characteristic (ROC) curve (AUC), sensitivity, and specificity were used to evaluate the performance of Model 1. The standard answer of the three experts, as mentioned above, was obtained using an online annotator. Model 2 used a bounding box to annotate lesions, and as long as there was one box bounding lesion, the model's detection of the current image was considered correct.

**Assessment of ResNet-50**

In the image test set, lesion images abstracted from original images according to the standard answer obtained by the three experts mentioned above were

used to assess the performance of Model 2. Accuracy, sensitivity, and specificity were used to evaluate the models.

**Assessment with the retrospective video test set and comparison with endoscopists**

We evaluated the overall performance of the proposed system on the video test set. Model 1 detected lesions with bounding boxes and Model 2 classified the boxed lesions, and the output classification results were recorded. Three experts provided standard answers for this video test set and we evaluated ENDOANGEL-DBE's performance in terms of accuracy, sensitivity, and specificity. The videos were cropped by 25 frames per second, and the lesions were boxed by Model 1 and then input into Model 2 for classification. The models provided a diagnosis every second, and the final result of a video was obtained from the largest proportion of all the diagnoses from the video.

Four novices with less than 10 cases of DBE experience and an additional 4 experts with more than 200 cases of DBE experience participated in a human and machine contest. The 4 experts in the video test were different from the 3 experts who developed the standard answers. They diagnosed the same 65 videos independently. The test in ENDOANGEL-DBE was performed 8 times to compare the results with those 8 endoscopists.

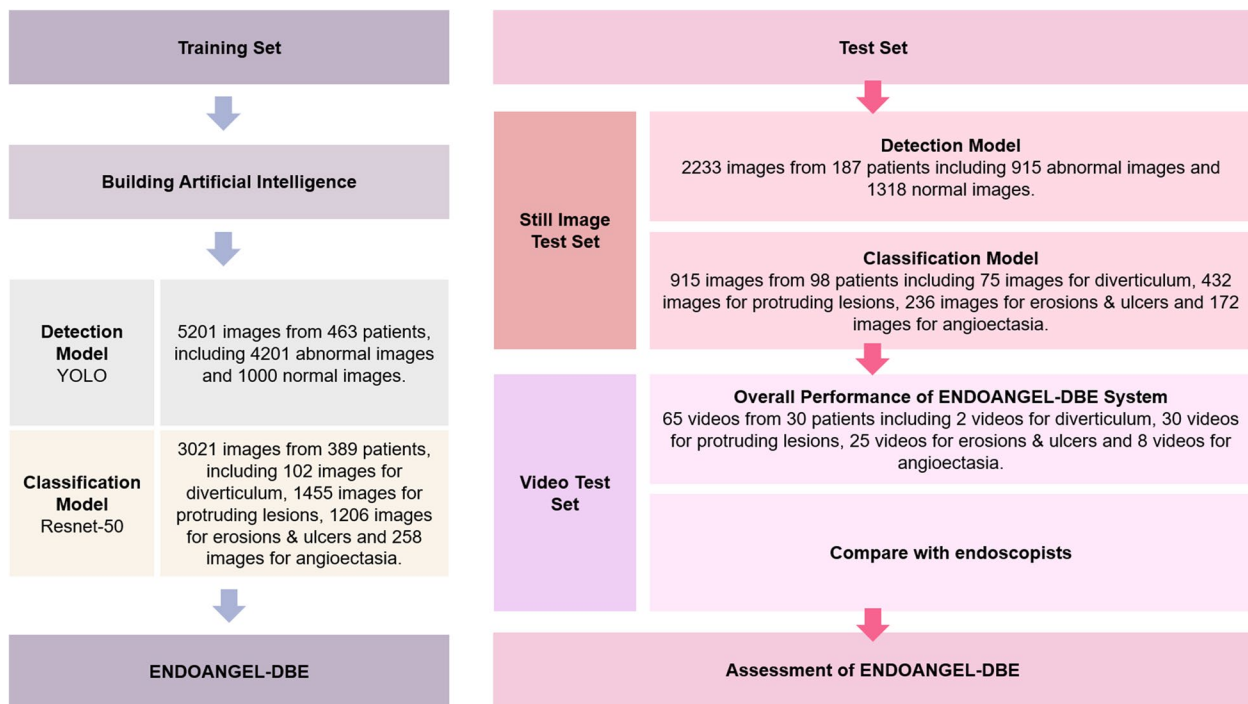


**Fig. 2** Flow chart

### Statistical analysis

Continuous variables are shown as the mean and standard deviation. McNemar's test was used for comparisons between ENDOANGEL-DBE and the endoscopists. All calculations were performed using SPSS 26 (IBM, Chicago, Illinois, USA).

### Ethics

The Ethics Committee approved this study at RHWU. The Ethics Committees waived informed consent in this retrospective study. Patient information was hidden during training and testing.

## Results

### Performance of ENDOANGEL-DBE for images

The AUC of Model 1 for the image test set was 0.947. The ROC curve is shown in Supplementary Fig. 1. The sensitivity of Model 1 in detecting lesions was 92% and the specificity was 93%. Ninety-eight out of 1318 normal images in the image test set were recognized as abnormal images, and 72 out of 915 abnormal images had no box bounding lesion. Normal mucosa, mucus, feces, light spots, dim spots, bubbles, and dark view induced false-positive results. Normal mucosa was the primary contributor to false-positive images. Most of the false-negative images were misjudged owing to dark view, lesions resembling the surrounding mucosa, and lesions with small flat haematin bases (Table 1).

Typical images for classification are shown in Supplementary Fig. 2. The overall accuracy of Model 2 was 86%. The sensitivity of classifying protruding lesions was 93%, which was the highest among the four common lesions, and the lowest sensitivity was 80% (erosions & ulcers and diverticulum). ENDOANGEL-DBE also achieved high performance in classifying

**Table 1** False positive images & false negative images analysis in the image test set

	Misjudged reasons	Number of images
<b>False positive images</b>	Normal mucosa	53
	Mucus & faeces	18
	Light spot & dim & bubbles	24
	Dark view	3
<b>False negative images<sup>a</sup></b>	Diverticulum	33
	Erosion & Ulcer	15
	Protruding lesion	19
	Angioectasia	5

<sup>a</sup> Most of the false negative images were misjudged by the following factors: dark view, lesions that are similar to surrounding mucosa and few of lesions with small flat hematin base

angioectasia in the image test set (85%). The specificity of classifying diverticulum was 99%.

### Performance of ENDOANGEL-DBE for videos

There were 65 videos in the video test set. The detection sensitivity was 100% in the per-case analysis and 93% in the per-frame analysis. The total classification accuracy of ENDOANGEL-DBE was 85%. The number of correct cases that ENDOANGEL-DBE and human observe for different classes of lesions is shown in Table 2. The performance of ENDOANGEL-DBE for the video test set is shown as a confusion matrix in Supplementary Fig. 3.

### Human and machine comparison

The total accuracy of endoscopists was 77%. The overall performance of ENDOANGEL-DBE was superior to that of endoscopists ( $p < 0.01$ ). Twenty out of 25 erosion & ulcer cases were diagnosed correctly by ENDOANGEL-DBE, and it had more correct cases than endoscopists in this class. The number of cases that ENDOANGEL and endoscopists diagnosed correctly in diverticulum and protruding lesions were comparable. In addition, the overall performance of ENDOANGEL-DBE was superior to that of novices (73%,  $p < 0.01$ ). ENDOANGEL diagnosed more correct cases than the novices did in classifying erosion & ulcer and angioectasia. The overall performance of ENDOANGEL was comparable to the experts in classification (81%;  $p = 0.253$ ). And it diagnosed more correct cases than experts did in classifying angioectasia. The number of correct cases that ENDOANGEL and experts diagnosed correctly was comparable in classifying the other three lesion classes (Table 2). A demonstration video is shown in Video 1.

In this video test, some erosion and angioectasia cases were confused. ENDOANGEL-DBE misdiagnosed three angioectasia cases as erosions and one erosion as angioectasia. One protruding lesion was misdiagnosed as a diverticulum because of peristalsis (Fig. 3).

**Table 2** The number of correct cases diagnosed by endoscopists and ENDOANGEL-DBE in video test set. The results of endoscopists are shown as averages  $\pm$  standard deviations

	ENDOANGEL-DBE	Endoscopists	Experts	Novices
<b>Diverticulum</b>	2	2.0 $\pm$ 0.0	2.0 $\pm$ 0.0	2.0 $\pm$ 0.0
<b>Protruding lesion</b>	27	27.6 $\pm$ 0.9	27.8 $\pm$ 0.4	27.5 $\pm$ 1.1
<b>Erosion &amp; ulcer</b>	20	15.6 $\pm$ 4.6	13.5 $\pm$ 1.9	17.8 $\pm$ 5.5
<b>Angioectasia</b>	6	4.9 $\pm$ 1.5	4.5 $\pm$ 1.1	5.3 $\pm$ 1.7



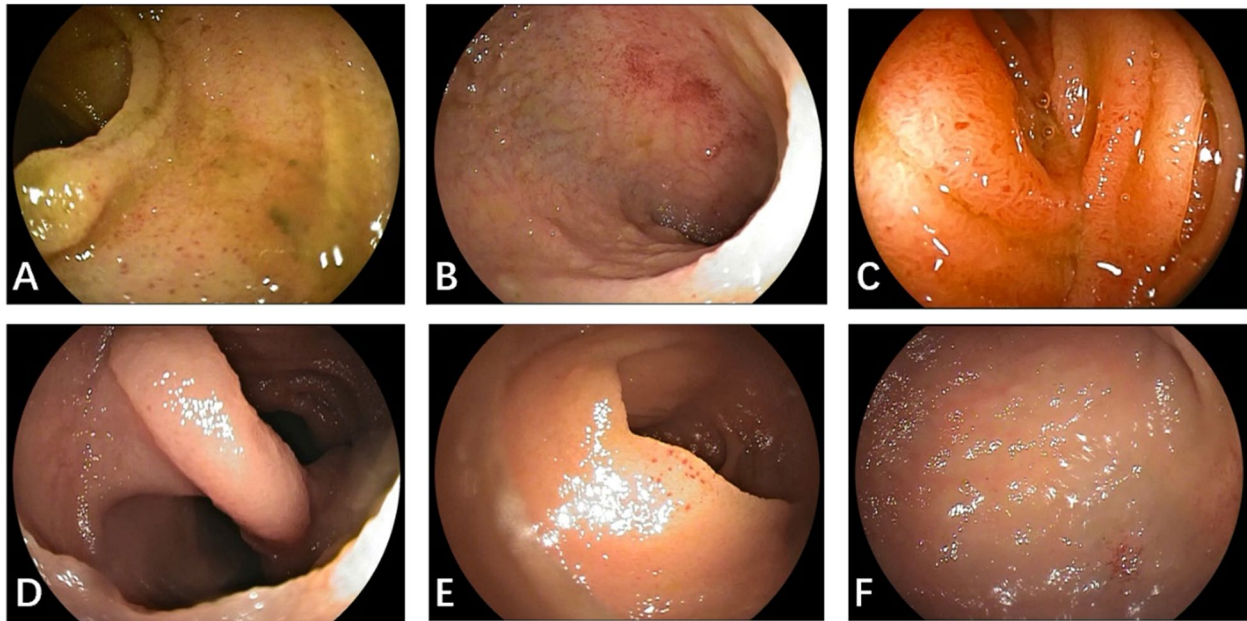


**Fig. 3** Misdiagnosed cases of machine or endoscopists. **A** Erosions misdiagnosed as angioectasia by novices because bile affects observation. **B** small erosions misdiagnosed as angioectasia by novices. **C** Angioectasia with red background misdiagnosed as erosion&ulcer by machine and novices. **D** Pedunculated polyps in the lumen during peristalsis misdiagnosed as diverticulum by machine. **E** small angioectasia misdiagnosed as erosion&ulcer by machine. **F** angioectasia in the edge of view misdiagnosed as erosion&ulcer by machine

## Discussion

The promising performance of CNN-based AI algorithms on CE images inspired us to explore their utility in image analysis in the field of DBE images.

In this study, we developed a CNN-based system to automatically recognize and classify small bowel lesions. This is the first study to develop a CAD system and evaluate it with both DBE images and videos. The CAD system performed similar to experts' evaluations and better than novices. It might be a useful tool, to improve diagnostic yield in DBE, especially for novices. ENDOANGEL-DBE has the potential to reduce missed lesions, interoperator variability, and improve diagnostic accuracy for common small bowel lesions. Another potential application of ENDOANGEL-DBE is in DBE training. Automatic detection and classification CNN programs can assist in image reading training via real-time feedback, which may shorten the training time and accelerate experience accumulation for trainees. Furthermore, the classification model of this CAD system will facilitate further exploitation towards an automatic diagnosis and reporting system for DBE examination.

Automatic detection assists in reducing the miss rate of four common lesions instead of a single type, and classification will be finished after detecting them, which is one of the advantages of our study compared with previous studies [50–52]. Our system has reached a high accuracy in detecting and classifying small bowel lesions.

To reduce false-positive cases, we used normal images as noise in the training set of the detection model, and we achieved satisfactory results. Notably, we found that ENDOANGEL-DBE's diagnostic precision of erosion & ulcer was the lowest among the four classes of lesions for both the image and video test sets. Most of the misdiagnosed cases were small, red, and spot lesions, especially those with a red background. The targeted collection of small erosion and angioectasia images for further training improvement is necessary to improve ENDOANGEL-DBE diagnostic performance. In the video test set, dark view and red background were the main reasons for false-positive results for ENDOANGEL-DBE. Transfer learning will be used to decrease false-positive cases in further studies. In this video test, the main reason for endoscopists' misdiagnosis is that the lesions are small, the background in the video is red in tone and bile can also affect observation. We found that ENDOANGEL-DBE diagnosed more correct cases than experts in diagnosing angioectasia in the video test set. Since there were only eight cases of angioectasia included in this video test set, we need further validation in larger test sets to make the results comparable.

Recent studies have shown that the sensitivity of AI in single disease classification under device-assisted enteroscopy has reached 88.5–97% [50–52]. Their training set included more images than our study, but the number of recruited cases in these studies was less than that

in ours. Increasing the number of recruited cases will improve the generalizability of the system. These studies were only based on images and our study also assessed ENDOANGEL-DBE's performance with videos. Miguel Martins et al. [51] developed a model recognizing erosions and ulcers from normal images, whose sensitivity was higher than ours. Since they did not use an independent test set, the images in their test set and training set might come from the same cases, and using such a test set might lead to higher results than those in the real world. These studies aim to detect one single type of lesions, but our system can detect and classify multiple types of lesions. AI systems for automatic detection and classification under CE achieved accuracy of 88.2–100% [31, 33, 34, 53]. These studies contained very large training sets and reached a high detection accuracy. Referring to the above research, we could attempt to use multiple binary classification models or enrich our training sets to further improve our system.

Several limitations of this study must be acknowledged. First, this is a single-centre retrospective study, and only endoscopists from RHWU participated. We should conduct a larger test among endoscopists from different hospitals to compare the performance of the CAD system and humans. We will also plan a multicentre prospective clinical trial to assess its performance in daily clinical routines. Second, the standard answer of this study is expert consensus instead of pathology. The model development was strongly dependent on the consensus of the three experts, which were humans. This study mainly focuses on endoscopic diagnosis. A comprehensive diagnostic system combining pathological and clinical results will be constructed in future studies. Additionally, to further improve our system, model selection, dataset revision, and cross-validation will be used for model training. Third, to make the comparison results fair, the endoscopists were told that the test cases were one of the four types of lesions. However, this might lead to a higher diagnostic accuracy of endoscopists than that in clinical diagnosis. A further comparison between endoscopists with and without AI in unclipped videos is needed to investigate the influence of AI. Fourth, lesions might be missed when multiple different lesions appear at the same time during examinations because of the distance from endoscopy and lesion size. ENDOANGEL-DBE needs further training using multiple lesion images for clinical use. This system will be improved to make diagnoses and assess their relevance to bleeding in future studies. Furthermore, we can develop a system with a positioning function in the future, which can pinpoint the location of lesions. The system can be trained for the assessment of lesion size and the detection of obscure

small intestinal bleeding. It could also be used to write an automatic report, which will lessen the administrative workload of endoscopists.

## Conclusions

In conclusion, we developed a novel computer-aided diagnostic system for small bowel lesions in DBE. This CAD system can assist especially novice endoscopists in increasing their diagnostic yield.

## Abbreviations

DBE	Double-balloon enteroscopy
CAD	Computer-aided diagnostic
AUC	Area under the curve
CE	Capsule endoscopy
AI	Artificial intelligence
CNN	Convolutional neural network
RHWU	Renmin Hospital of Wuhan University
VAI	VGG Image Annotator
ROC	Receiver operating characteristic
DAE	Device-assisted enteroscopy

## Supplementary Information

The online version contains supplementary material available at <https://doi.org/10.1186/s12876-023-03067-w>.

### Additional file 1.

**Additional file 2: Video 1.** This is a demonstration video of how the system ENDOANGEL-DBE works. Real-time bounding boxes will appear when the system detects a lesion, and its class is shown on the left side of the screen. ENDOANGEL-DBE will generate a heatmap when the image is stable.

## Acknowledgements

This work was partly supported by the grant from Innovation Team Project of Health Commission of Hubei Province (grant no. WJ202C003) (to Honggang Yu). The funder had no role in study design, data collection, data analysis, data interpretation, or writing of the report. The corresponding author had full access to all the data in the study and had final responsibility for the decision to submit for publication.

## Authors' contributions

HGY and LZ conceived and designed the study; ANY, FL, YW collected images and baseline information. ANY, FL, XT and LLW reviewed images; JXW, MJZ, LH, CXZ, XDJ and DXG participated in the competition with the model; YJZ and XGL collected, collated and analyzed the data; LZ and YJZ wrote the manuscript; SH guided algorithm; LLW and XT contributed to algorithm development; HGY and LZ performed extensive editing of the manuscript; all authors reviewed and approved the final manuscript for submission. All authors were involved in data acquisition, general design of the trial, interpretation of the data, and critical revision of the manuscript. #, \*These authors contribute equally to this work. All authors contribute to critical revision of the manuscript.

## Funding

This work was partly supported by the grant from Innovation Team Project of Health Commission of Hubei Province (grant no. WJ202C003) (to Honggang Yu).

## Availability of data and materials

Individual de-identified participant data that underlie the results reported in this article and study protocol will be shared for investigators after article publication. To gain access, data requesters will need to contact the corresponding author.

## Declarations

### Ethics approval and consent to participate

The Ethics Committee of Renmin Hospital of Wuhan University (No: WDRY2019-K073) approved the study. The requirement for informed consent was waived by the Ethics Committee of Renmin Hospital of Wuhan University because of the retrospective nature of the study. The study was performed in accordance with the Declaration of Helsinki.

### Consent for publication

Not applicable.

### Competing interests

The authors declare no competing interests.

### Author details

<sup>1</sup>Department of Gastroenterology, Renmin Hospital of Wuhan University, Wuhan, China. <sup>2</sup>Key Laboratory of Hubei Province for Digestive System Disease, Renmin Hospital of Wuhan University, Wuhan, China. <sup>3</sup>Hubei Provincial Clinical Research Center for Digestive Disease Minimally Invasive Incision, Renmin Hospital of Wuhan University, Wuhan, China. <sup>4</sup>School of Computer Science, Wuhan University, Wuhan, China.

Received: 8 April 2023 Accepted: 28 November 2023

Published online: 02 January 2024

## References

- Chauhan SS, Manfredi MA, Abu Dayyeh BK, Enestvedt BK, Fujii-Lau LL, Komanduri S, et al. Enteroscopy. *Gastrointest Endosc.* 2015;82(6):975–90.
- Kim JS, Kim BW. Training in endoscopy: esophagogastroduodenoscopy. *Clin Endosc.* 2017;50(4):318–21.
- May A. Double-balloon Enteroscopy. *Gastrointest Endosc Clin N Am.* 2017;27(1):113–22.
- Aniwan S, Viriyautsahakul V, Luangsukrerk T, Angsuwatcharakon P, Piyachaturawat P, Kongkam P, et al. Low rate of recurrent bleeding after double-balloon endoscopy-guided therapy in patients with overt obscure gastrointestinal bleeding. *Surg Endosc.* 2021;35(5):2119–25.
- Gomes C, Rubio Mateos JM, Pinho RT, Ponte A, Rodrigues A, Fosado Gayosso M, et al. The rebleeding rate in patients evaluated for obscure gastrointestinal bleeding after negative small bowel findings by device assisted enteroscopy. *Rev Esp Enferm Dig.* 2020;112(4):262–8.
- Hashimoto R, Matsuda T, Nakahori M. False-negative double-balloon enteroscopy in overt small bowel bleeding: long-term follow-up after negative results. *Surg Endosc.* 2019;33(8):2635–41.
- Shinozaki S, Yano T, Sakamoto H, Sunada K, Hayashi Y, Sato H, et al. Long-term outcomes in patients with overt obscure gastrointestinal bleeding after negative double-balloon endoscopy. *Dig Dis Sci.* 2015;60(12):3691–6.
- Guo Y, Liu Y, Oerlemans A, Lao S, Wu S, Lew MS. Deep learning for visual understanding: a review. *Neurocomputing.* 2016;187:27–48.
- Krizhevsky A, Sutskever I, Hinton GE. ImageNet classification with deep convolutional neural networks. *Commun ACM.* 2017;60(6):84–90.
- Kumar P, Manash E. Deep learning: a branch of machine learning. *J Phys Conf Ser.* 2019;1228:012045.
- LeCun Y, Bengio Y, Hinton G. Deep learning. *Nature.* 2015;521(7553):436–44.
- Russell SJ, Norvig P. *Artificial intelligence. a modern approach.* Third ed. Pearson; 2014.
- Bibault J-E, Giraud P, Burgun A. Big data and machine learning in radiation oncology: state of the art and future prospects. *Cancer Lett.* 2016;382(1):110–7.
- Cruz-Roa A, González FA, Gilmore H, Basavanahally A, Feldman M, Shih NNC, et al. Accurate and reproducible invasive breast cancer detection in whole-slide images: a deep learning approach for quantifying tumor extent. *Sci Rep.* 2017;7:46450.
- Ehteshami Bejnordi B, Veta M, Johannes van Diest P, van Ginneken B, Karssemeijer N, Litjens G, et al. Diagnostic assessment of deep learning algorithms for detection of lymph node metastases in women with breast Cancer. *Jama.* 2017;318(22):2199–210.
- Esteve A, Kuprel B, Novoa RA, Ko J, Swetter SM, Blau HM, et al. Dermatologist-level classification of skin cancer with deep neural networks. *Nature.* 2017;542(7639):115–8.
- Gulshan V, Peng L, Coram M, Stumpe MC, Wu D, Narayanaswamy A, et al. Development and validation of a deep learning algorithm for detection of diabetic retinopathy in retinal fundus photographs. *Jama.* 2016;316(22):2402–10.
- Larson DB, Chen MC, Lungren MP, Halabi SS, Stence NV, Langlotz CP. Performance of a deep-learning neural network model in assessing skeletal maturity on pediatric hand radiographs. *Radiology.* 2018;287(1):313–22.
- Ting DSW, Cheung CY, Lim G, Tan GSW, Quang ND, Gan A, et al. Development and validation of a deep learning system for diabetic retinopathy and related eye diseases using retinal images from multiethnic populations with diabetes. *Jama.* 2017;318(22):2211–23.
- Topol EJ. High-performance medicine: the convergence of human and artificial intelligence. *Nat Med.* 2019;25(1):44–56.
- Yasaka K, Akai H, Kunimatsu A, Abe O, Kiryu S. Liver fibrosis: deep convolutional neural network for staging by using Gadoteric acid-enhanced hepatobiliary phase MR images. *Radiology.* 2018;287(1):146–55.
- Chahal D, Byrne MF. A primer on artificial intelligence and its application to endoscopy. *Gastrointest Endosc.* 2020;92(4):813–20.e4.
- Le Berre C, Sandborn WJ, Aridhi S, Devignes MD, Fournier L, Smail-Tabbone M, et al. Application of artificial intelligence to gastroenterology and Hepatology. *Gastroenterology.* 2020;158(1):76–94.e2.
- Min JK, Kwak MS, Cha JM. Overview of deep learning in gastrointestinal endoscopy. *Gut Liver.* 2019;13(4):388–93.
- Sinonquel P, Eelbode T, Bossuyt P, Maes F, Bisschops R. Artificial intelligence and its impact on quality improvement in upper and lower gastrointestinal endoscopy. *Dig Endosc.* 2021;33(2):242–53.
- Suzuki H, Yoshitaka T, Yoshio T, Tada T. Artificial intelligence for cancer detection of the upper gastrointestinal tract. *Dig Endosc.* 2021;33(2):254–62.
- Li J, Zhu Y, Dong Z, He X, Xu M, Liu J, et al. Development and validation of a feature extraction-based logical anthropomorphic diagnostic system for early gastric cancer: a case-control study. *EClinicalMedicine.* 2022;46:101366.
- Takenaka K, Ohtsuka K, Fujii T, Oshima S, Okamoto R, Watanabe M. Deep neural network accurately predicts prognosis of ulcerative colitis using endoscopic images. *Gastroenterology.* 2021;160(6):2175–7.e3.
- Wu L, Zhang J, Zhou W, An P, Shen L, Liu J, et al. Randomised controlled trial of WISENSE, a real-time quality improving system for monitoring blind spots during esophagogastroduodenoscopy. *Gut.* 2019;68(12):2161–9.
- Zhou J, Wu L, Wan X, Shen L, Liu J, Zhang J, et al. A novel artificial intelligence system for the assessment of bowel preparation (with video). *Gastrointest Endosc.* 2020;91(2):428–35.e2.
- Aoki T, Yamada A, Aoyama K, Saito H, Tsuboi A, Nakada A, et al. Automatic detection of erosions and ulcerations in wireless capsule endoscopy images based on a deep convolutional neural network. *Gastrointest Endosc.* 2019;89(2):357–63.e2.
- Aoki T, Yamada A, Kato Y, Saito H, Tsuboi A, Nakada A, et al. Automatic detection of blood content in capsule endoscopy images based on a deep convolutional neural network. *J Gastroenterol Hepatol.* 2020;35(7):1196–200.
- Aoki T, Yamada A, Kato Y, Saito H, Tsuboi A, Nakada A, et al. Automatic detection of various abnormalities in capsule endoscopy videos by a deep learning-based system: a multicenter study. *Gastrointest Endosc.* 2021;93(1):165–73.e1.
- Ding Z, Shi H, Zhang H, Meng L, Fan M, Han C, et al. Gastroenterologist-level identification of small-bowel diseases and Normal variants by capsule endoscopy using a deep-learning model. *Gastroenterology.* 2019;157(4):1044–54.e5.
- Fan S, Xu L, Fan Y, Wei K, Li L. Computer-aided detection of small intestinal ulcer and erosion in wireless capsule endoscopy images. *Phys Med Biol.* 2018;63(16):165001.
- He J-Y, Wu X, Jiang Y-G, Peng Q, Jain R. Hookworm detection in wireless capsule endoscopy images with deep learning. *IEEE Trans Image Process.* 2018;27(5):2379–92.



37. Klang E, Barash Y, Margalit RY, Soffer S, Shimon O, Albshesh A, et al. Deep learning algorithms for automated detection of Crohn's disease ulcers by video capsule endoscopy. *Gastrointest Endosc.* 2020;91(3):606–13.e2.
38. Noorda R, Nevárez A, Colomer A, Pons Beltrán V, Naranjo V. Automatic evaluation of degree of cleanliness in capsule endoscopy based on a novel CNN architecture. *Sci Rep.* 2020;10(1):17706.
39. Noya F, Alvarez-Gonzalez MA, Benitez R. Automated angiodysplasia detection from wireless capsule endoscopy. *Annu Int Conf IEEE Eng Med Biol Soc.* 2017;2017:3158–61.
40. Saito H, Aoki T, Aoyama K, Kato Y, Tsuboi A, Yamada A, et al. Automatic detection and classification of protruding lesions in wireless capsule endoscopy images based on a deep convolutional neural network. *Gastrointest Endosc.* 2020;92(1):144–51.e1.
41. Tsuboi A, Oka S, Aoyama K, Saito H, Aoki T, Yamada A, et al. Artificial intelligence using a convolutional neural network for automatic detection of small-bowel angioectasia in capsule endoscopy images. *Dig Endosc.* 2020;32(3):382–90.
42. Wang S, Xing Y, Zhang L, Gao H, Zhang H. A systematic evaluation and optimization of automatic detection of ulcers in wireless capsule endoscopy on a large dataset using deep convolutional neural networks. *Phys Med Biol.* 2019;64(23):235014.
43. Yuan Y, Meng MQ. Deep learning for polyp recognition in wireless capsule endoscopy images. *Med Phys.* 2017;44(4):1379–89.
44. Dutta A, Zisserman A. The VIA annotation software for images, audio and video. In: *Proceedings of the 27th ACM International Conference on Multimedia (MM '19)*, October 21–25, 2019, Nice, France. New York: ACM; 2019. p. 4. <https://doi.org/10.1145/3343031.3350535>.
45. Redmon J, Divvala S, Girshick R, Farhadi A. You only look once: Unified, real-time object detection. In: *Proceedings of the IEEE conference on computer vision and pattern recognition*; 2016. p. 779–88.
46. Bernal J, Tajkbaksh N, Sanchez FJ, Matuszewski BJ, Chen H, Yu L, et al. Comparative validation of polyp detection methods in video colonoscopy: results from the MICCAI 2015 endoscopic vision challenge. *IEEE Trans Med Imaging.* 2017;36(6):1231–49.
47. Pacal I, Karaboga D. A robust real-time deep learning based automatic polyp detection system. *Comput Biol Med.* 2021;134:104519.
48. Qadir HA, Shin Y, Solhusvik J, Bergsland J, Aabakken L, Balasingham I. Toward real-time polyp detection using fully CNNs for 2D Gaussian shapes prediction. *Med Image Anal.* 2021;68:101897.
49. He K, Zhang X, Ren S, Sun J. Deep residual learning for image recognition. In: *Proceedings of the IEEE conference on computer vision and pattern recognition*; 2016. p. 770–8.
50. Mascarenhas Saraiva M, Ribeiro T, Afonso J, Andrade P, Cardoso P, Ferreira J, et al. Deep Learning and Device-Assisted Enteroscopy: Automatic Detection of Gastrointestinal Angioectasia. *Medicina.* 2021;57(12):1378.
51. Martins M, Mascarenhas M, Afonso J, Ribeiro T, Cardoso P, Mendes F, et al. Deep-learning and device-assisted enteroscopy: automatic panendoscopic detection of ulcers and erosions. *Medicina.* 2023;59(1):172.
52. Cardoso P, Saraiva MM, Afonso J, Ribeiro T, Andrade P, Ferreira J, et al. Artificial intelligence and device-assisted Enteroscopy: automatic detection of enteric protruding lesions using a convolutional neural network. *Clin Transl Gastroenterol.* 2022;13(8):e00514.
53. Otani K, Nakada A, Kurose Y, Niikura R, Yamada A, Aoki T, et al. Automatic detection of different types of small-bowel lesions on capsule endoscopy images using a newly developed deep convolutional neural network. *Endoscopy.* 2020;52(9):786–91.

## Publisher's Note

Springer Nature remains neutral with regard to jurisdictional claims in published maps and institutional affiliations.

Ready to submit your research? Choose BMC and benefit from:

- fast, convenient online submission
- thorough peer review by experienced researchers in your field
- rapid publication on acceptance
- support for research data, including large and complex data types
- gold Open Access which fosters wider collaboration and increased citations
- maximum visibility for your research: over 100M website views per year

At BMC, research is always in progress.

Learn more [biomedcentral.com/submissions](https://biomedcentral.com/submissions)

